Allen *et al. Energy Mater* 2024;4:400037
DOI: 10.20517/energymater.2023.111

Energy Materials

Review

Open Access

Check for updates

A theoretical review of passivation technologies in perovskite solar cells

Oscar J. Allen, Jian Kang, Shangshu Qian, Jack J. Hinsch, Lei Zhang*, Yun Wang*

Centre for Catalysis and Clean Energy, School of Environment and Science, Gold Coast Campus, Griffith University, Queensland 4222, Australia.

***Correspondence to:** Prof. Yun Wang, Centre for Catalysis and Clean Energy, School of Environment and Science, Gold Coast Campus, Griffith University, 1 Parklands Drive, Southport, Queensland 4222, Australia. E-mail: yun.wang@griffith.edu.au; Dr. Lei Zhang, Centre for Catalysis and Clean Energy, School of Environment and Science, Gold Coast Campus, Griffith University, 1 Parklands Drive, Southport, Queensland 4222, Australia. E-mail: lei.zhang@griffith.edu.au

How to cite this article: Allen OJ, Kang J, Qian S, Hinsch JJ, Zhang L, Wang Y. A theoretical review of passivation technologies in perovskite solar cells. *Energy Mater* 2024;4:400037. https://dx.doi.org/10.20517/energymater.2023.111

Received: 22 Dec 2023 **First Decision:** 5 Mar 2024 **Revised:** 25 Mar 2024 **Accepted:** 11 Apr 2024 **Published:** 22 Apr 2024

Academic Editors: Meicheng Li, Weihua Tang **Copy Editor:** Fangyuan Liu **Production Editor:** Fangyuan Liu

Abstract

Perovskite solar cells have demonstrated remarkable progress in recent years. However, their widespread commercialization faces challenges arising from defects and environmental vulnerabilities, leading to limitations in energy conversion efficiency and device stability. To overcome these hurdles, passivation technologies have emerged as a promising avenue. These passivators are strategically applied at the interface between perovskite absorbers and charge transport layers to mitigate the adverse effects of defects and environmental factors. While prior reviews have predominantly focused on experimental observations, a comprehensive theoretical understanding of the passivators has been lacking. This review focuses on recent advancements in first-principles density functional theory studies that delve into the fundamental properties of passivators and their intricate interactions with perovskite materials and charge transport layers. By exploring the atomic-level roles of passivators, this review elucidates their impact on critical parameters such as open circuit voltage (V_{oc}), short circuit current density (J_{sc}), fill factor, and the overall stability of perovskite solar cells. The synthesis of theoretical insights from these studies can serve as guidelines for the molecular design of passivators with the ultimate objective of advancing the commercialization of high-performance perovskite solar cells.

Keywords: Perovskite solar cells, passivation, density functional theory, open circuit voltage, short circuit current density, fill factor, stability

INTRODUCTION

Over the last decade, remarkable strides have been achieved in the field of perovskite solar cells (PSCs), establishing them as exceptionally promising contenders for widespread commercialization[1]. The distinctive optoelectronic characteristics of metal-halide perovskites, encompassing a high absorption coefficient, extended carrier diffusion lengths (L), and adaptable bandgaps, contribute to their remarkable efficacy in capturing and converting sunlight into electricity[1-3]. Additionally, using solution-based deposition methods for perovskite film formation presents the potential for large-scale, cost-effective manufacturing processes, underscoring PSCs as a promising technology for achieving widespread adoption of renewable energy[4,5]. To date, PSCs have achieved impressive power conversion efficiencies (PCEs) exceeding 25% in both normal n-i-p and inverted p-i-n structures in laboratory settings, rapidly approaching the theoretical Shockley-Queisser efficiency limit[3]. Nonetheless, some challenges still need to be addressed before their commercial adoption.

A significant hindrance is the inherent formation of defect-trapping states during the fabrication of PSCs, with these defects exerting a pronounced negative impact on overall device performance and resulting in diminished PCEs[6-8]. Additionally, the degradation of perovskite light absorbers under diverse environmental factors, such as moisture, poses another significant challenge for PSC commercialization[9,10]. The susceptibility of perovskite materials to these external factors can lead to decreased efficiency over time, limiting their practical applicability. To position PSCs as a highly competitive and sustainable technology for solar energy conversion, their long-term stability (LTS) and reliability must be meticulously addressed to ensure consistent performance over extended operational periods.

To address the challenges associated with defect formation and light absorber degradation during PSC operation, substantial efforts have been devoted to developing passivation techniques[11]. These techniques aim to either suppress the formation of defects or enhance the stability of the light absorbers, thereby improving the overall performance of PSCs. Passivators are commonly introduced at the interface between the perovskite light absorbers and the charge transport layers, including the electron transport layer (ETL) and the hole transport layer (HTL) [Figure 1A]. Strategically incorporating passivators into the device architecture can reduce the defect density within the perovskite layer or between interfaces, significantly enhancing carrier recombination dynamics and charge extraction efficiency. Consequently, the key parameters related to the energy conversion performance of PSCs, including open-circuit voltage (V_{OC}), short-circuit current density (J_{SC}), and fill factor (FF), can be substantially improved. Determination of these parameters involves measuring and analyzing the current-voltage (J-V) characteristics of the device [Figure 1B]. Furthermore, passivation techniques exhibit promise in extending the lifespan of perovskite light absorbers by mitigating the detrimental effects of environmental factors, such as moisture, thereby preserving the structural integrity and optoelectronic properties of perovskite materials. This enhanced stability is crucial for the long-term performance and durability of PSCs, facilitating their practical implementation in real-world applications.

Various passivators and passivation technologies have been explored in the realm of PSCs. Potential passivators encompass cation and anions dopants[12], one- (1D)[13] or two-dimensional (2D) materials[14], Lewis acid-based adducts[15], alkylammonium halogen salts[16], and hydrophobic organic molecules[17]. Several comprehensive review papers have delved into the properties and potential applications of these passivation materials[6,18,19]. However, the full atomic-level impact of passivators on solar cell performance remains challenging to grasp solely through experimental results, owing to the limitations of characterization techniques. In this regard, theoretical investigations offer a valuable supplement to experimental studies, offering the potential to unveil the structure-function-performance relationship of

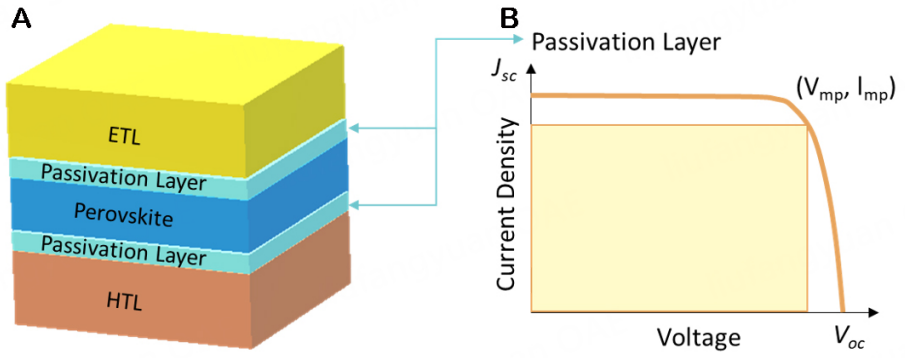

Figure 1. (A) Illustration of the structure of perovskite solar cells, including ETL, perovskite light absorbers and HTL. The passivation layer is introduced to improve the energy conversion parameters. Three important parameters, including V_{OC}, J_{SC}, and FF, are shown in (B) the J-V curve.

passivators. Surprisingly, the theoretical understanding of the function of passivators in PSCs has received a scant review, primarily because most theoretical studies have been integrated into literature employing a combined experimental and theoretical approach. Relatively few independent theoretical studies on this topic have been conducted and systematically summarized.

To fill this knowledge gap, we consolidate existing theoretical knowledge to facilitate the translation of theoretical insights into practical applications. In this review, we present an overview of computational methods used in theoretical studies on passivators and passivation techniques in PSCs. Recent examples are utilized to elucidate the theoretical understanding of passivation in enhancing energy conversion efficiency, including improvements in V_{OC}, J_{SC}, and FF. This review also addresses the role of passivators in prolonging the lifetime of PSCs. Drawing on recent theoretical advances, selection criteria are then proposed for designing PSC passivators.

METHODOLOGIES

Density functional theory

Density functional theory (DFT) is a widely employed method for investigating the structure-function-performance relationship of passivators in PSCs due to its computational efficiency and acceptable accuracy[20-26]. In DFT, the exact form of exchange-correlation (XC) functional is unknown, necessitating approximations. A common DFT approach involves using semi-local XC functionals with the generalized gradient approximation (GGA)[13,14]. However, conventional DFT methods at the GGA level often fall short of accurately capturing van der Waals (vdW) forces. Prior research highlights the critical role of precise vdW force treatment in describing the structural properties of PSC materials, particularly in the presence of heavy elements such as Pb and I[27-29]. Therefore, incorporating vdW correction in the DFT method becomes essential.

Furthermore, DFT at the GGA level tends to underestimate the bandgap of semiconductors[30-33]. While GGA-level calculations can replicate the bandgap of certain organic-lead perovskite materials, their band structures become inaccurate without accounting for spin-orbit coupling (SOC) effects[34-37]. SOC arises from the interaction between the magnetic dipole of an electron and the electric field generated by atomic nuclei, becoming prominent in heavy atoms due to relativistic effects. For instance, SOC calculations on $MAPbI_3$ reveal band splitting, resulting in a significantly smaller bandgap compared to experimental

values[38,39]. Additionally, the positions of the conduction band minimum (CBM) and valence band maximum (VBM) are notably altered, affecting the optical properties and effective masses of charge carriers. Therefore, accurate evaluation of electronic and optical properties in theoretical studies necessitates the consideration of SOC effects[38,40-63]. After considering the SOC, the calculated bandgap of $MAPbI_3$ is significantly smaller than the experimental value. To produce more accurate electronic properties, a hybrid functional including a fraction of exact non-local Hartree-Fock (HF) exchange was introduced[12]. To this end, the accurate electronic and optical properties of lead (Pb)-based perovskite light absorbers can only be achieved using the hybrid DFT method with the consideration of the SOC effect. It should be noted that hybrid DFT calculations considering the SOC effect are computationally intense, and most theoretical studies on passivation techniques tend to neglect this effect due to its minimal influence on structural and energetic properties[64].

Theoretical parameters related to V_{oc}

The V_{OC} refers to the voltage generated by a solar cell in the absence of current flow due to a broken circuit or exceptionally high resistance. Theoretically, it corresponds to the energy difference between the CBM and VBM levels when considering only the light absorbers in the solar cell. In solar cell devices, ETLs and HTLs are utilized to facilitate the separation and efficient transfer of photo-generated electrons (e^-) and holes (h^+), reducing their recombination. Typically, when an electron is photo-excited from the valence band (VB) to the conduction band (CB), photoelectrons transfer from the CB of the absorber to the CB of the ETL, while photo-holes migrate from the VB of the absorber to the VB of the HTL. To enable the effective transfer of photoelectrons from the light absorber to the ETL, the CBM of the ETL should be lower than that of the perovskite materials. Similarly, the VBM of the HTL should be higher than that of the light absorber, guiding the movement of photo-holes from the absorber to the HTL. Consequently, the theoretical V_{OC} value of the device becomes the difference between the CBM of the ETL and the VBM of the HTL.

The CBM and VBM levels can be theoretically determined through the DFT calculation. The CBM and VBM locations can be calculated with respect to the vacuum energy level (E_{vac}). The E_{vac} can be calculated by averaging the electrostatic potential along the normal direction of the surface. For metallic materials, there are no CBM and VBM. Instead, the work function (Φ) is used to represent the highest occupied energy level of the surface. The band structure analysis can further identify the CBM and VBM associated with k-vectors. In direct semiconductors, CBM and VBM share the same k-vector, while in indirect band gap materials, their k-vectors are different. It is worth noting that band structure calculations at the DFT-GGA level can result in severe underestimations of the CBM, leading to a significant reduction of 30% to 40% in the overall bandgap[30-33]. To address this, hybrid DFT methods incorporating HF exchange have been shown to provide more accurate theoretical bandgap, CBM and VBM results[65].

Theoretical parameters related to J_{sc}

The J_{SC} represents the maximum current density achievable by a cell when operating under negligible resistance and zero voltage. In the context of solar cells, the electrical conductivity of the materials used, such as the passivation layer, can influence the J_{SC} value. Higher electrical conductivity allows for better charge transport, which results in higher current densities under short-circuit conditions. By understanding the relationship between the J_{SC} and the electrical conductivity of passivation materials, researchers can make informed choices in material selection and device design to enhance the performance of solar cells. Therefore, optimizing the electrical conductivity of the materials within a solar cell can help maximize the J_{SC} and overall device performance.

The Drude model provides a valuable tool for estimating and predicting electrical conductivity behaviors, thereby aiding in developing more efficient solar cell technologies. In this model, conductivity depends on parameters such as carrier concentration (n), charge (e), and mobility (m)[66]. The concentration of carriers is influenced by the density of defects and the inherent ability to generate carriers. The carrier mobility, on the other hand, is affected by the *L* of charge carriers. The *L* values are determined by the effective mass of the exciton (m^*)[67]. The m^* value can be theoretically calculated using

$$m^* = \hbar^2 \left[\frac{\partial^2 \varepsilon(k)}{\partial k^2}\right]^{-1} \quad (1)$$

where $\hbar$ represents the reduced Planck's constant, k denotes the wave vector along different directions, and $\varepsilon(k)$ refers to the eigenvalue of the energy band, which can be obtained from DFT calculations.

Previous studies underscore the necessity of considering the SOC effect for accurately predicting effective masses, particularly in materials with heavy elements[34]. The incorporation of SOC in the calculations increases the band dispersions, resulting in reduced effective masses for both electrons and holes. For example, Umari *et al.* investigated the effective masses of electrons and holes of $MAPbI_3$ using different methods[68]. Without accounting for SOC, the average effective masses were 0.73 m_0 for electrons and 0.36 m_0 for holes (m_0 is the free electron mass). Upon introducing the SOC effect, the effective masses were significantly reduced to 0.17 m_0 for electrons and 0.28 m_0 for holes, attributing this reduction to the existence of heavy elements such as Pb and I. However, most passivators consist of relatively light elements that lack a significant SOC effect. Consequently, the computation of exciton effective masses for passivators often neglects the SOC effect because of its high computation cost.

The J_{SC} of a solar cell also heavily depends on the optical properties of the device and is directly proportional to the power of the incident light. Therefore, the absorption and light-harvesting capabilities of the solar cell play a crucial role in determining J_{SC}. Enhancing the optical properties, including enhanced light absorption and minimized reflection or transmission losses, can increase J_{SC}. To this end, an effective passivator should exhibit low reflectivity and absorption, minimizing its impact on the light absorption by the perovskite materials. To assess this, the absorption coefficients ($\alpha(\omega) \times 10^5$ cm^{-1}) and optical reflectivity ($R(\omega)$) can be calculated from complex dielectric function ($\varepsilon(\omega) = \varepsilon_1(\omega) + i\varepsilon_2(\omega)$) using

$$R(\omega) = \frac{(n-1)^2+k^2}{(n+1)^2+k^2} \quad (2)$$

$$\alpha(\omega) = \frac{\sqrt{2}\omega}{c}\left[\frac{\sqrt{\varepsilon_1^2+\varepsilon_2^2}+\varepsilon_1}{2}\right]^{1/2} \quad (3)$$

Theoretical parameters related to FF

The FF is utilized to determine the maximum power output of a solar cell. This maximum power point (P_{MP}) corresponds to the ideal voltage (V_{mp}) and current density (J_{mp}) at which the solar cell operates most efficiently, maximizing its power generation (See Figure 1B). The FF can be improved by increasing $P_{MP,}$

which can be achieved by enhancing the charge collection efficiency[69]. The charge collection efficiency in solar cells is influenced by the charge transfer between different layers. The binding strength between specific layers within the solar cell structure plays a crucial role. A strong binding between the layers efficiently facilitates charge transfer (electrons and holes) across interfaces, minimizing charge recombination losses. In this regard, the charge collection efficiency can be improved by optimizing the binding strength between these layers, leading to enhanced overall performance of the solar cell.

The binding strength between molecular passivators can be evaluated based on their adsorption energy (ΔE_{ad}) on the perovskite material surfaces. The ΔE_{ad} is calculated by

$$\Delta E_{ad} = (E_{ad/surf} - E_{surf} - n \times E_{ad})/n \quad (4)$$

where E_{ad}, E_{surf}, and $E_{ad/surf}$ are the energies of the passivator, the clean perovskite surface, and the perovskite surface with passivators, respectively, and n is the number of passivators in each surface cell.

For the 2D materials, their binding strength (ΔE_b) can be calculated by

$$\Delta E_b = (E_{hybrid} - E_{surf} - E_{2D})/A \quad (5)$$

where E_{2D} and E_{hybrid} are the energies of 2D monolayer and their interface with 2D monolayers on perovskite surface, respectively. The A is the area of the interface within each unit cell.

Theoretical parameters related to stability

Mitigating the instability of halide perovskites under operational conditions is a crucial objective in the field of PSCs[70]. One of the primary challenges in achieving this stability lies in preventing the adsorption of water, which can degrade the perovskite material over time[71]. To address this issue, passivators act as protective layers to block the pathways for water adsorption. By introducing passivators that have a stronger affinity to the perovskite surface than water, their adsorption can outcompete that of water molecules. This competitive adsorption prevents the undesired interaction of water with the perovskite material and maintains its stability during operation.

To assess the performance of passivation, it is crucial to evaluate the effectiveness of the passivator compared to water adsorption. This evaluation can be conducted through theoretical investigations using DFT calculations. By employing theoretical investigations and assessing the competitive adsorption of passivators with water, researchers can gain insights into the potential of diverse passivators to protect halide perovskites from degradation under operational conditions. Therefore, theoretical calculations can provide valuable guidance in designing and selecting effective passivation strategies. The DFT at the GGA level often allows researchers to simulate and predict the adsorption behavior of molecules and materials at the atomic level[72]. By calculating the adsorption or binding energies using Eq. 4 and 5, the passivation performance of different passivator candidates can be quantitatively assessed. Since the negative adsorption energy values suggest the exothermic process, a lower adsorption energy indicates a stronger interaction between the passivator and the perovskite surface, suggesting a more effective passivation strategy.

PASSIVATION FOR IMPROVING V_{oc}

The optimization of band alignment between the ETL/HTL and perovskite light absorbers is crucial for improving the V_{OC} in PSCs. To achieve optimal band alignment, passivators need to possess energy levels that bridge the gap between the HTL/ETL and the perovskite absorbers. The ideal alignment of band edges for efficient photovoltaic applications is not always naturally achieved due to the inherent electronic properties of the materials. Misalignment between the charge transport layers and light absorbers can result in internal voltage drops (IVDs), reducing the theoretical V_{OC}[73-78]. Thus, passivation strategies aim to modify the CBM and VBM positions, as illustrated in Figure 2A.

In recent studies, the effectiveness of passivators in improving the V_{OC} of PSCs has been demonstrated through theoretical investigations and experimental validations. Various passivation approaches have been proposed and investigated in recent studies, including surface passivation[79], interface engineering[80], defect passivation[81,82], and composition optimization[83]. Each approach has specific challenges associated with band misalignment in PSCs. Theoretical investigations using DFT calculations provide valuable insights into the band structures of passivated layers within solar cells, allowing for the design and evaluation of effective passivation strategies.

Passivation at the adsorber-ETL interface

Che *et al.* systematically studied the effect of carbonyl, hydrazine and phenyl groups in different passivators using three kinds of hydrazide derivatives (benzoyl hydrazine (BH), formohydrazide (FH), and benzamide (BA))[84]. Their DFT calculations at the GGA level reveal that the carboxyl and hydrazine groups in BH can effectively interact with surface Pb^{2+}, employing a synergistic double coordination approach. This interaction passivates both shallow- and deep-level defects by increasing the energy barrier for lattice distortion. The adsorption of BH passivators can lead to a noteworthy increase in the CBM energy level of $CsPbI_3$, resulting in a corresponding increase in the V_{OC} from 1.17 to 1.24 V. Zhang *et al.* investigated the role of acetylcholine (ACh^+) on enhancing the V_{OC} of PSCs[85]. Combining experimental and theoretical approaches, their DFT calculations at the Perdew-Burke-Ernzerhof (PBE)-GGA level focused on the electronic properties of the $MAPbI_3$ (100) surface. Density of states (DOS) analyses unveiled the presence of Pb-I antisites and I vacancies, introducing deep and shallow trap states in the band gap, consequently diminishing the V_{OC}. However, after the adsorption of ACh^+ on the defective sites, both deep and shallow trap states were successfully removed or reduced. The results indicated that introducing ACh^+ reduced the surface energies of the MA-I and Pb-I terminated surfaces, leading to the passivation of surface defect states. As a result, both the deep and shallow trap states can be efficiently removed, as evidenced by the DOS analysis [Figure 2B and C]. The DOS images further support the increase of the CBM after removing defect states, providing a rationale for the observed increase in V_{OC} from 1.12 to 1.21 V after the passivation with ACh^+.

Dong *et al.* also demonstrated that chlorobenzenesulfonic potassium salts can interact with uncoordinated tin ions in tin oxide ETL[86]. Calculations done with PBE-GGA and DFT-D3 revealed that the carbon-chlorine bonds in the salts filled tin oxide oxygen vacancies, improving band-level alignment. Consequently, the V_{OC} shifted from 1.127 V toward an ideal value, 1.163 V. Furthermore, Batmunkh *et al.* employed passivators to enhance the V_{OC} by tuning the CBM of the ETL in the n-i-p device[87]. In their study, the introduction of single-wall carbon nanotubes (SWCNTs) between TiO_2 ETL and perovskite increased the V_{OC} from 0.87 to 0.93 V. First-principles DFT calculations at the GGA-PBE level revealed that the CBM level of TiO_2 ETL increased by 0.23 V upon SWCNT adsorption on the anatase TiO_2 (101) surface, as shown in Figure 2D. This increased CBM location of the ETL aligns with the experimental observations, resulting in an enhanced theoretical V_{OC}. Additionally, Chavan *et al.* explored passivation on the ETL to

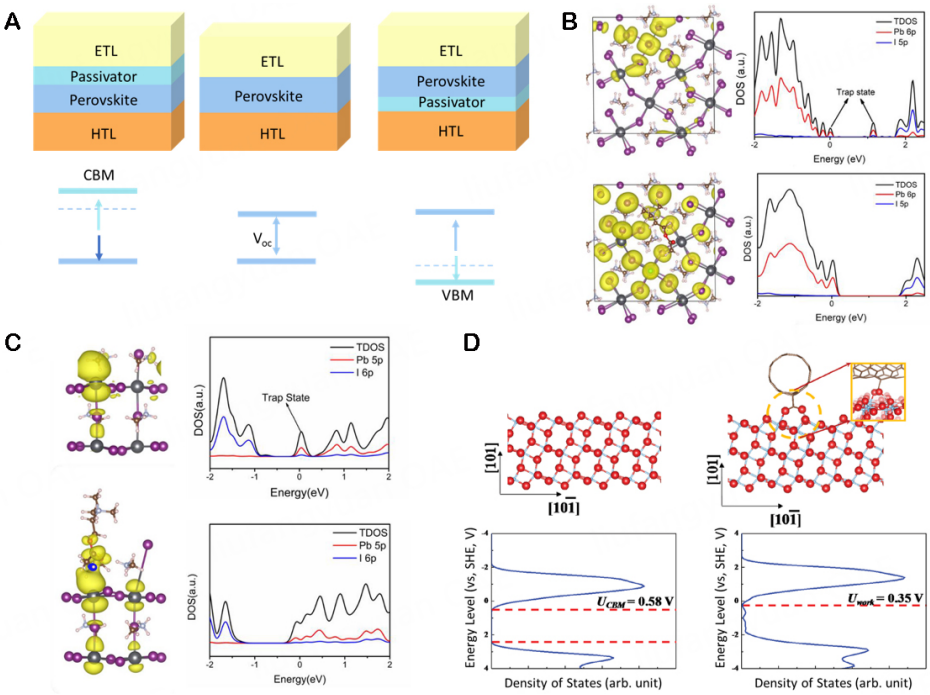

Figure 2. (A) Illustration of the role of the ideal passivator at the interface between ETL and perovskite materials or between HTL and perovskite materials to change the CBM or VBM locations, respectively to further improve the V_{OC}. (B) The passivator Cs^+ was used to fill the MA^+ vacancy, leading to decreased VBM location of the perovskites and increased V_{OC}[85]. Copyright 2022 Wiley. (C) The use of ACh^+ passivators to fill the MA^+ vacancy leads to removing the deep trap states, as evidenced by the DOS analysis[85]. Copyright 2022 Wiley. (D) The use of ACh^+ passivators to fill the MA^+ vacancy leads to removing the shallow trap states, as evidenced by the DOS analysis[87]. Copyright 2017 Wiley.

enhance the V_{OC} by improving band-level alignment[88]. Large bandgap oxides, such as Nb_2O_5 and Ta_2O_5, were investigated to suppress surface defects. This study examined ultraviolet photoelectron spectroscopy and Mott-Schottky measurements to determine the electron conditions. While Nb_2O_5 passivations lightly increased the V_{OC} from 1.118 to 1.147 V, the introduction of Ta_2O_5 led to a further improvement in V_{OC} to 1.16 V. Theses tudies highlight the significance of passivators in modulating band alignment andsuppressing defect states in PSCs, ultimately improving V_{OC} and overall device performance.

Passivation at the adsorber-HTL interface

Jiang *et al.* reported that surface engineering by using 3-(amino methyl) pyridine (3-APy) as a passivator can efficiently reduce the perovskite surface roughness and surface potential fluctuations associated with the surface states[89]. Moreover, the negatively charged pyridine rings in the 3-Apy passivator can react with the surface formamidinium (FA) ions. DFT calculations at the GGA level reveal that this reaction facilitates the formation of surface iodine vacancies, enabling n-type doping. As a result, the VBM of the perovskite experienced a notable shift from 0.80 to 1.51 eV, explaining the enhanced V_{OC} of 1.19 V in the experiments. Bati *et al.* used Cs-doped $Ti_3C_2T_x$ MXene as a passivator in PSCs[90]. Their DFT calculations at the GGA level with an optB86b vdW correction method showed the formation of an MA^+ cation vacancy in the $MAPbI_3$ perovskite, which led to a shift in the VBM from -5.88 to -5.60 V to the E_{vac}. However, the subsequent adsorption of Cs^+ at the MA^+ vacancy restored the VBM to -5.90 V. This shift in the VBM can be attributed to the strong adsorption of Cs^+ with an adsorption energy of -5.13 eV, effectively eliminating defect states caused by the absence of MA^+ on the surface. The introduction of Cs-doped $Ti_3C_2T_x$ MXene resulted in an enhanced V_{OC} from 1.05 to 1.10 V, highlighting the role of the VBM shift in providing device performance.

Zhang *et al.* also discovered a passivating material to increase the charge carrier lifetimes and improve band-level alignments[91]. Here, the PBE-GGA method was used to understand the electronic conditions. They used the electron-dense benzene ring of Boc-S-4-methoxy-benzyl-L-cysteine (BMBC) to strengthen interactions with undercoordinated lead ions. These mechanisms improved band edge alignments to increase the V_{OC} from 1.144 to 1.249 V. On top of this, Zhang *et al.* have used trifluoroacetamidine for defect suppression, again with the PBE functional[92]. Here, hydrogen bonds from the fluorine groups interacted with the perovskite to reduce recombination. The reduction in recombination rates at the grain boundaries allowed the V_{OC} to be brought up from 1.10 to 1.16 V.

PASSIVATION FOR IMPROVING J_{SC}

In contrast to the extensive research on passivation for improving V_{OC}, both experimental and theoretical investigations on the passivation effect on J_{SC} are relatively rare. The J_{SC} values are influenced by various factors, including the presence of defects and the optical properties of the solar cell. Defects can affect J_{SC} by influencing the minority-carrier collection probability. Their presence can create recombination centers that reduce the efficiency of collecting minority carriers, leading to a decrease in J_{SC}. To this end, various passivation strategies have been proposed to enhance light absorption, minimize recombination, and optimize charge carrier collection efficiency to increase J_{SC}. Accordingly, the theoretical studies on passivation mainly focus on suppressing charge recombination rates.

Batmunkh *et al.* employed phosphorene (P) nanosheets as passivators to improve carrier mobilities in planar n-i-p PSCs[93]. Utilizing DFT calculations at the PBE-GGA level for initial atomic structure optimization and subsequent hybrid DFT calculations with the HSE06 functional for accurate electronic properties, the CBM position of 5-layer phosphorene was found to bridge between the CBM of TiO_2 ETL and the perovskite. This band alignment indicated that phosphorene could act as a bridge between the ETL and the light absorber, facilitating the transfer of photo-excited electrons, reducing charge recombination rates, and increasing J_{SC} [Figure 3A-C]. Experimental results showed a modest increase in J_{SC} from 22.21 to 23.32 mA/cm^2 after introducing phosphorene passivators. The effectiveness of using black phosphorene as a passivator to improve J_{SC} has also been experimentally confirmed by Macdonald *et al.*[94].

Inspired by the experimental results, Allen *et al.* further conducted DFT calculations at the hybrid HSE06 level to investigate the effective mass of various Group VA monolayers, including black phosphorene from their band structures [Figure 3D][95]. The results showed that Group VA monolayers have small effective masses of charge carriers, indicating promise for their use as passivators for both ETL and HTL interfaces. Notably, Cheng *et al.* predicted high hole mobility for 2D β-antimony, and HSE06 results indicated that all α-group VA monolayers effectively facilitate charge transfer due to their low effective masses[96]. Most β-group VA monolayers have relatively higher effective masses compared to silicon, except for β-Sb and β-Bi in terms of hole transport. This observation implies that both α and β-phase group VA monolayers typically exhibit high mobility as semiconductors. This characteristic facilitates accelerated charge transport, attributable to their low intrinsic mobility of holes and electrons. Figure 3E illustrates that both α- and β-phases of P and arsenene (As) monolayers have low reflectivity in the visible light range across all directions. Conversely, antimonene (Sb) and bismuthene (Bi) monolayers, particularly in their α-phases, exhibit high reflectivity to visible light. Therefore, incorporating Sb and Bi monolayers as passivators in solar cells may lead to decreased absorbed light by the perovskite light absorbers. Additionally, DFT results indicate that α-Sb and Bi monolayers have large absorption coefficients for visible light [Figure 3F], further restricting the exposure of visible light to the light absorbers in solar cells. Although β-Sb and Bi have smaller absorption coefficients, their values remain relatively high. Therefore, caution is recommended when using Sb and Bi monolayers as passivators due to their unfavorable optical properties. In comparison,

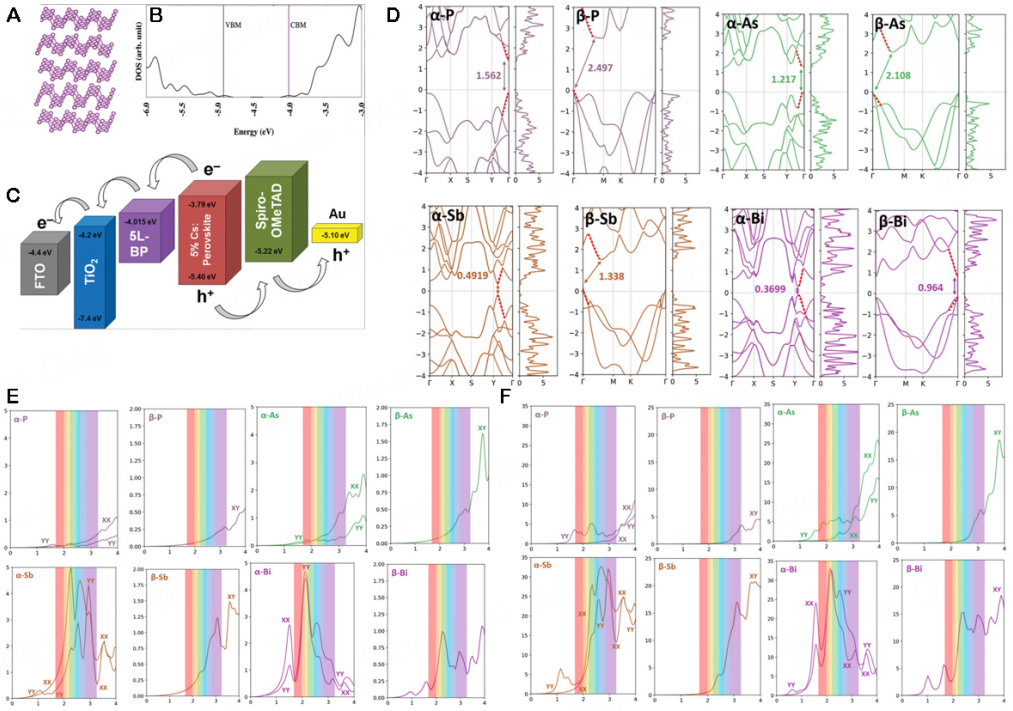

Figure 3. (A) The atomic structure and (B) density of states of five-layer phosphorene, shifted with respect to the vacuum level E_V. The vertical purple lines indicate the positions of the CBM and VBM. (C) Energy diagram of five-layer phosphorene incorporated TiO_2 photoelectrodes-based PSC[93]. Copyright 2019 Wiley. (D) Band structures and TDOS of phosphorene (P), arsenene (As), antimonene (Sb), and bismuthine (Bi) with α-phase and β-phase. The dashed lines indicate the direction for calculating the effective masses of electrons and holes[95]. Copyright 2023 American Chemical Society. (E) Simulated reflectivity (R(ω)) spectra of phosphorene (P), arsenene (As), antimonene (Sb), and bismuthine (Bi) with the α-phase and β-phase[95]. Copyright 2023 American Chemical Society. (F) Calculated absorption coefficients (α(ω) × 105 cm^{-1}) of phosphorene (P), arsenene (As), antimonene (Sb), and bismuthine (Bi) with the α-phase and β-phase[95]. Copyright 2023 American Chemical Society.

P and As monolayers have lower absorption coefficients in the visible light range. However, their absorption coefficients are higher than that of the TiO_2 ETL and similar to perovskite materials such as $MAPbI_3$. This indicates that P and As monolayers should be avoided in the light pathway to the light absorbers. In the standard inverted p-i-n PSC configuration, it is preferable to incorporate them between the ETL and perovskite. Conversely, in the standard n-i-p configuration, these passivators are favored between the HTL and light absorbers.

PASSIVATION FOR IMPROVING FF

The FF is a critical parameter that significantly influences the overall efficiency of a solar cell. It represents the extent to which the actual power output of the cell approaches the maximum theoretical power. Therefore, improving the FF is essential to enhance the overall performance of the solar cell. One effective strategy to boost the FF is to increase the anchoring strength between the various components of the cell. Reinforcing the interlayer interactions and bonds among different materials can minimize energy losses, improve charge carrier transport, and consequently enhance the FF within the device. To quantify the interlayer anchoring strengths, researchers mainly rely on quantitative theoretical measurements, such as analyzing the binding energies of the layers involved. These measurements provide valuable insights into the stability and cohesion between the different layers, contributing to the design and development of solar cells with improved FF and enhanced overall efficiency. Similar to the V_{OC}, FF is heavily related to interlayer interaction. Consequently, the location of passivation can be either at the adsorber-ETL or adsorber-HTL interface, as illustrated in Figure 4A.

Passivation at the adsorber-ETL interface

Li *et al.* introduced phenethylammonium (PEA) cations, 4-Fluorophenethylammonium (F-PEA)), and 4-(Trifluoromethyl) phenethylammonium (CF3-PEA) with the distinct dipole moments to the interface between inorganic $CsPbI_{3-x}Br_x$ perovskite light absorber layer and C_{60}/ALD-SnO_2 ETL[97]. Initially, they used the hybrid B3LYP DFT method with D3 vdW correction to calculate the electrostatic potentials of these passivators. Subsequently, DFT computations at the hybrid level with Heyd–Scuseria–Ernzerhof (HSE) functional and D3 vdW corrections were conducted. They found that CF3-PEA can have a stronger interaction with the light absorbers and C60 due to its high polarity. As a result, it significantly facilitated charge transfer between light absorbers and ETL, contributing to improving the FF from 80.7% to 82.8%. Xu *et al.* used the DFT at the GGA-PBE level to investigate a 2-mercapto-1-methylimidazole passivator[98]. This material was found to form lead-sulfur bonds, reinforcing the interface. This strengthening resulted in fewer defect states and improved energy alignments, leading to an overall increase in the FF from 81.3% to 83.6%.

Qiao *et al.* conducted a study to investigate the impact of Sb or In cation doping on $Cs_{0.1}FA_{0.9}PbI_3$ PSCs, achieving an impressive FF of 84.0% by optimizing fabrication parameters[99]. To understand the underlying mechanisms, they performed theoretical analysis using DFT calculations at the PBE-GGA level with D3 vdW correction. Their theoretical analysis revealed that introducing Sb or In cations in the interlayers of the solar cell strengthened the interlayer interactions. The adsorption energies of PbI_4, InI_3, and SbI_4 on the TiO_2 ETL surface were determined to be -0.81, -0.89 and -0.90 eV, respectively, indicating the stability and favorable binding of the dopant cations to the TiO_2 surface. This observation was supported by the corresponding I-Ti bond distances of 3.30, 3.28 and 3.25 Å when PbI_4, InI_3, and SbI_4 were adsorbed, respectively. Further analysis of the partial DOS (PDOS) indicated a minimal overlap between Pb 6s and O 2p states, suggesting limited hybridization between these states. Similarly, weak hybridization was found between I 6p and Ti 3d states. However, in the interface with Sb or In cations, the analysis revealed enhanced hybridization between the cations' 5s orbitals and the O 2p orbitals within the antibonding energy range. Furthermore, the hybridization between the I 6p orbitals and the Ti 3d orbitals was strengthened after doping [Figure 4B]. This enhanced hybridization indicates a stronger interaction between the antimony or indium cations and the surrounding atoms. Charge density difference plots [Figure 4C] provided further evidence of the effects of doping, demonstrating increased charge transfer across the interface between the Sb cation-based cluster and the anatase TiO_2 (101) surface. This stronger hybridization between the antimony or indium cations-based clusters and the TiO_2 ETL surface greatly facilitates interface charge transfer, resulting in improved FF [Figure 4D]. The highest FF was observed in the Sb-doped PSC, reaching 84%. This was followed by an FF of 76% in the In-doped PSC. In comparison, the undoped Pb-based PSC exhibited an FF of 71%. The theoretical analysis shed light on the beneficial effects of Sb or In cation doping. These dopants improved interlayer interactions, resulting in improved charge transport and, ultimately, higher FF values in the fabricated PSCs.

Recently, Zhang *et al.* provided a guanidinium hydrochloride passivator that improves the FF[100]. The DFT results suggest that this passivator decreased the deep-level trap defects through the strong adsorption on the SnO_2 ETL, such as the oxygen vacancy and unsaturated coordinated surface Sn atoms. Especially, the binding energy of the guanidinium hydrochloride on the SnO_2 surface is 4.31 eV. Their DOS analysis demonstrates that both Sn 5p and Pb 6p states in guanidinium hydrochloride-passivated SnO_2 and perovskite surfaces are similar to those in defect-free SnO_2 and perovskite. Consequently, the passivation can reduce the trap density with reduced nonradiative recombination at this interface. This led to better electron transport with an improved FF of 81.81% from 77.72%.

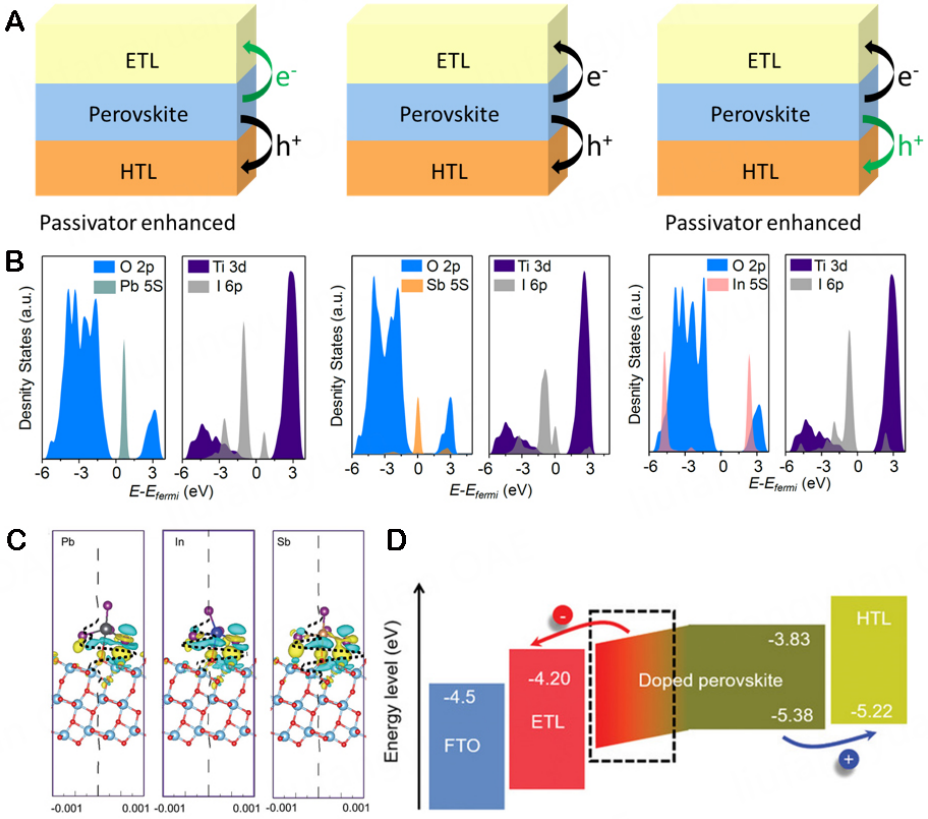

Figure 4. (A) Illustration of the role of passivation layers on FF. The green arrow indicates the enhanced charge transfer rate due to the stronger interactions between different layers. (B) PDOS of the interface between (left) pristine, (middle) Sb^{3+} doped and (right) In^{3+} doped $Cs_{0.1}FA_{0.9}PbI_3$ perovskite films with TiO_2[99]. Copyright 2018 Wiley. (C) Theoretical simulation of charge density. (left) The charge density at the interface between the Pb^{2+}-based cluster, (middle) the In^{3+}-based cluster, and (right) the Sb^{3+}-based cluster (C) and the anatase TiO_2 (101) surface, respectively[99]. Copyright 2018 Wiley. (D) Schematic diagram of band shift of perovskite and TiO_2 in graded heterojunction structure with a mixed and graded interlayer. The negative and the positive circles represent electrons and holes, respectively, and the arrows express their flowing directions[99]. Copyright 2018 Wiley.

Passivation at the adsorber-HTL interface

Liu *et al.* recently identified 1,3-bis(diphenylphosphino)propane (DPPP) as an effective passivator for improving the FF[101]. Employing DFT computations at the PBE-GGA level with the D3 vdW correction, the authors screened different Lewis bases and determined that P exhibited the highest binding affinity with the perovskite surface. Consequently, DPPP was selected as the promising passivators, demonstrating a tight interaction with surface Pb^{2+} with a binding energy of 2.24 eV. More importantly, DPPP exhibited a robust interaction with NiO_x HTL, with the binding energy increasing to 4.31 eV upon spontaneous interaction with the perovskite surface and NiO_x HTL. These strong interactions between the light absorber layer and HTL lead to an increased FF, observed in the experimentally from 79% to 82%. Fei *et al.* investigated the adsorption properties of bathocuproine (BCP) on the perovskite surface compared to the widely used dimethyl sulfoxide (DMSO) perovskite precursor solvent[102]. Utilizing the DFT computation at the PBE-GGA level with D3 vdW correction, they determined that BCP exhibited stronger adsorption, effectively disrupting the surface Pb-Pb dimer and eliminating associated deep gap states. Based on the DFT results, BCP was used as lead chelation molecules (LCMs) at the interface between the perovskite layer and PTAA HTLs. Competing with DMSO for lead ions through strong chelation, BCP reduced DMSO residue and the amorphous region in perovskites near the HTLs. Experimental validation confirmed the DFT predictions, revealing that replacing DMSO with BCP can reduce the amorphous region in perovskites near the HTLs,

facilitating improved charge transfer. Consequently, the FF value increased from 80.3% to 82.5%. Zhang *et al.* highlighted the potential of BMBC for enhancing the FF[91]. They utilized DFT at the PBE-GGA level to reveal that the passivation of BMBC can significantly suppress the formation of iodine vacancies. The resultant enhancement in charge transfer was directly linked to an improved property at the perovskite-HTL interface, leading to an increased FF from 80.05% to 83.57%. Additionally, Xie *et al.* employed DFT to demonstrate FF improvement alongside other benefits[103]. Methoxy-substituted triphenylamine tris(2,4,6-trichlorophenyl) methyl was used to defect passivation, focusing on free radical-assisted chlorine groups and electron donating groups. The passivator improved band level alignment, benefiting the perovskite-HTL interface and increasing the initial FF of 77.2% FF to as high as 80.7%. Tan *et al.* have demonstrated that the uniformity of perovskites or charge-transport layers may significantly affect their PCE[104]. Based on the DFT computation results with the PBEsol XC functional and DFT-D3 vdW correction, they found a work-function shift promoting halide migration. Octylammonium iodide (OAI) treatment resulted in the most significant work-function alteration (from 4.67 to 4.49 eV) compared to octylammonium tosylate (OATsO) (4.77 eV). The theoretical results also revealed the electron accumulation at the HTL interface with OAI. The OATsO treatment was also shown to have better efficiency (and less hysteresis behavior) at 24.41% compared to the 22.8% efficiency of OAI.

When analyzing 2D materials, the adsorption is typically expressed in terms of single-layer adsorption rather than molecular adsorption. This means that the adsorption energy (E_{ads}) is converted to the binding energy (ΔE_b) by dividing it by the surface area (see Eq. 5). In the study conducted by Bati *et al.*, they experimentally observed that the introduction of Cs^+ dopants can increase the FF of the PSC with MXene from 71% to 76%[90]. Using the PBE-GGA method with the optB86b vdW correction, the DFT results provide theoretical insights into the role of Cs^+ doping. It was found that Cs^+ enhances the interaction strength between MXene and the perovskite film. The corresponding binding energy, indicating the strength of this interaction, is measured to be -0.016 eV/Å^2, which is 23% higher than the system without Cs^+. This increased interaction strength has led to the formation of a highly crystallized and improved morphology of the perovskite film. As a result, the defect density is effectively reduced. The stronger interaction between MXene and the perovskite film promotes charge transfer, thereby enhancing the FF values of the PSC.

PASSIVATION FOR IMPROVING STABILITY

The environmental stability of PSCs is a crucial aspect to consider, encompassing various factors. One area of foci for passivation techniques in perovskites is to improve their stability against moisture exposure. Physical surface passivation methods can be employed to isolate external layers, augmenting the hydrophobic properties of the cell to prevent water penetration and mitigate degradation. Additionally, cation doping serves as a strategy to enhance moisture resistance and overall stability in PSCs. Recent literature has highlighted several effective mechanisms to improve surface protection and enhance environmental stability. These mechanisms provide insights into strategies for preserving the integrity and performance of PSCs in challenging environmental conditions. By addressing issues related to moisture exposure, researchers aim to enhance the LTS and durability of PSCs for practical applications.

Yang *et al.* used the optB86b method with vdW correction to investigate the blocking effect of specific bulky organic cations on water pathways, revealing a prevention mechanism for water adsorption on the $CH_3NH_3PbI_3$ (100) surface due to steric hindrance, as shown in Figure 5A-C[105]. The presence of bulky organic cations caused a repositioning of surface iodine atoms, obstructing hydrate pathway formation. Based on the theoretical guidance, a novel water adsorption-blocking strategy was proposed, which significantly increased the lifespan of PSCs under moist conditions. The cells exhibited improved stability,

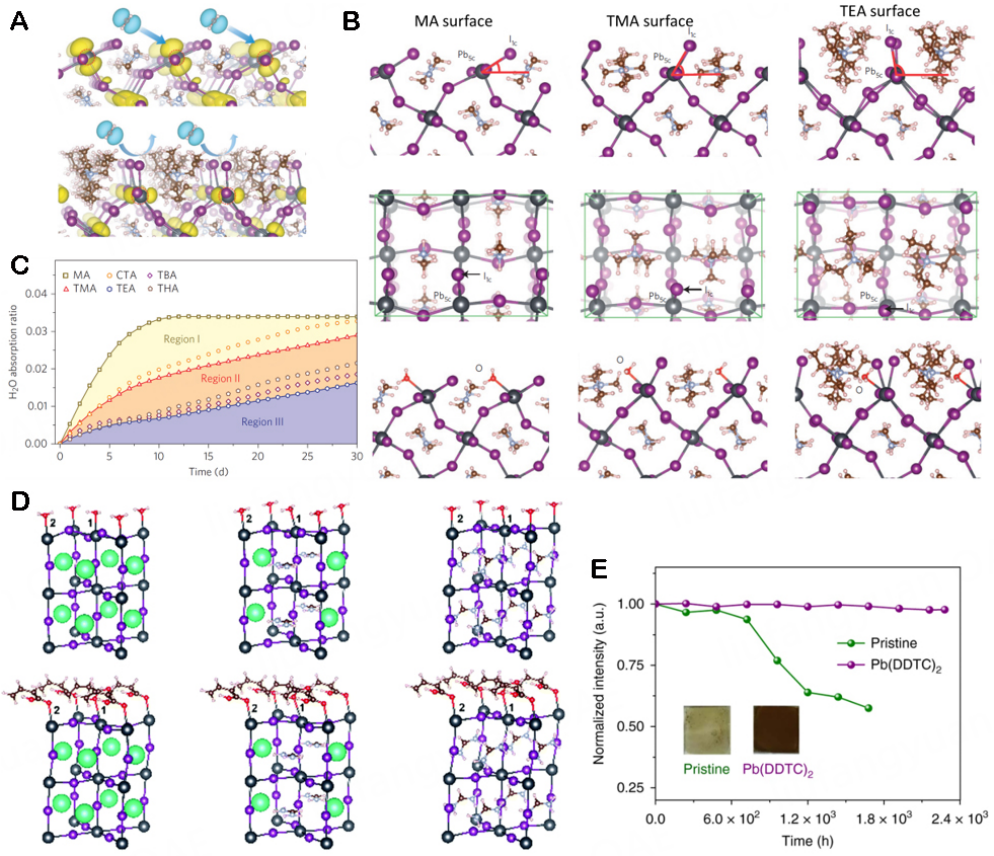

Figure 5. (A) Water molecule adsorption on perovskite surfaces. The MA (top) and TEA surfaces (bottom) are terminated with methyl and tetra-ethyl ammonium cations, respectively[105]. Copyright 2016 Nature Publishing Group. (B) Modeling atomic structures of functionalized perovskite surfaces. Side (top) and top (middle) views, respectively, of the optimized geometries of the (100) surfaces of MA, TMA and TEA samples. Calculated atomic structure (side view) of different (100) surfaces with molecularly adsorbed water (bottom)[105]. Copyright 2016 Nature Publishing Group. (C) Water absorption ratio of the perovskite crystals under a relative humidity of 90% ± 5% and dark conditions. Samples of more than 5 g were used in all tests for accuracy. Three regions are defined to classify the moisture resistance of all the samples[105]. Copyright 2016 Nature Publishing Group. (D) Atomic structures of $Cs_{1-x}FA_xPbI_3$ (001) surfaces with adsorbed H_2O and $C_4H_6O_2$ molecules in a unit cell: $CsPbI_3$ (left); $Cs_{0.5}FA_{0.5}PbI_3$ (middle); and $FAPbI_3$ (right)[64]. Copyright 2020 Royal Society of Chemistry. (E) Evolution of normalized absorbance for pristine (green) and chelated (purple, $Pb(DDTC)_2$) $CsPbI_2Br$ thin films under dark in ambient atmosphere (RH, 15% ± 3%)[106]. Copyright 2020 Nature Publishing Group.

with lifespans extending from mere seconds to an impressive 500 h in the presence of moisture, offering promising insights for practical application in diverse environmental conditions. Liu *et al.* conducted DFT computation at the GGA level with D3 vdW correction to investigate the interaction energies between water and 3-butenoic acid molecules on $Cs_{1-x}FA_xPbI_3$ (001) surfaces, where x represents the composition ratio (x = 0, 0.5, and 1)[64]. The study aimed to simulate forming a passivation layer on the perovskite surfaces by examining the adsorption of 3-butenoic acid with full coverage. The optimized adsorption structures of the molecules are depicted in Figure 5D. Structural optimization revealed adsorption onto undercoordinated surface Pb atoms, exploiting unoccupied p orbitals. Specifically, the oxygen atom of the carbonyl group in the 3-butenoic acid molecule formed a bond with the surface Pb atoms. The DFT results revealed that the adsorption energies (ΔE_{ad}) of the organic ligand on $CsPbI_3$, $Cs_{0.5}FA_{0.5}PbI_3$, and $FAPbI_3$ (001) surfaces were -0.90, -0.83, and -0.81 eV, respectively. These values were 0.36, 0.33, and 0.31 eV lower than the H_2O molecule on the corresponding surfaces. This study indicates that the adsorption strength of the organic molecule was approximately 150% stronger than that of water. Additionally, the study calculated the surface energy changes ($\Delta\gamma$) of all facets upon 3-butenoic acid adsorption. The $\Delta\gamma$ values were found to be -0.189, -0.168, and -0.159 J m^{-2} for $CsPbI_3$, $Cs_{0.5}FA_{0.5}PbI_3$, and $FAPbI_3$ (001) surfaces, respectively. These results demonstrated that the adsorption of 3-butenoic acid significantly reduced the surface energy. Consequently,

the surface passivation achieved by 3-butenoic acid effectively blocked water molecule adsorption, stabilizing the perovskite structure in a moist environment and aligning with experimental observations. He *et al.* investigated the passivation effects of dithiocarbamate on halide perovskites using the PBE-GGA functional in combination with DFT-D3 vdW corrections, considering the SOC[106]. Focusing on hindering water adsorption through steric hindrance, their calculations confirmed the effectiveness of dithiocarbamate in blocking water adsorption on the perovskite surface [Figure 5E]. The study offers valuable insights into passivation strategies for enhancing moisture stability in perovskite light absorbers.

Zhang *et al.* employed DFT calculations at the PBE-GGA level, incorporating the Tkatchenko-Scheffler vdW correction method, to explore the adsorption behavior of the phosphorene monolayer on the $MAPbI_3$ (001) surface[107]. They specifically examined two surface terminations: PbI-termination and bare-cation termination. Their findings indicated a stronger interaction between phosphorene and the PbI-terminated surface compared to the bare cation termination. This enhanced interaction was attributed to the larger attractions between the electron-rich phosphorus (P) atom in phosphorene and the electrophilic Pb atom in the perovskite surface. To evaluate the stability of perovskite materials protected by a phosphorene passivation layer, classical molecular dynamics (MD) simulations were employed. The MD results demonstrated that water molecules could easily approach both the PbI-terminated and cation-terminated perovskite surfaces. However, the surface passivation provided by phosphorene effectively blocked the adsorption of water molecules. This blocking effect can be attributed to the hydrophobic nature of phosphorene, which is consistent with experimental observations. This study highlighted the potential of phosphorene as a passivation layer to enhance the stability of perovskite materials by preventing water adsorption.

CONCLUSION AND REMAINING CHALLENGES

Passivation plays a crucial role in advancing efficient PSCs, aiming to enhance various aspects of their performance. Effective passivation mechanisms contribute to improved exciton transport, recombination prevention, and interlayer interactions. Progress has been notable in dopant, interfacial, and surface passivation techniques. Ongoing research focuses on refining passivation mechanisms, including exciton transport improvement, recombination prevention, interlayer anchoring, and moisture protection. A comprehensive understanding at the atomic scale is crucial for optimizing passivation strategies. This includes investigating the interactions between the passivator and perovskite material to improve V_{OC}, J_{SC}, and FF while exploring stability mechanisms to maintain high performance over time. Based on the recent theoretical studies, the selection criteria for a good passivator for PSCs from DFT computations can be summarized as follows:

i. Improvement of V_{OC}: The ideal passivator should align its CBM and VBM locations with the band structures of the perovskite light absorbers, ETL, and HTL. Additionally, the passivator should effectively suppress defect states, optimizing the band alignment between the perovskite light absorbers and charge transfer layers.

ii. Improvement of J_{SC}: Passivators should possess small charge-effective masses to facilitate efficient charge transfer. They should also exhibit low absorption and reflectivity coefficients in the visible light range, enabling a higher amount of incident light to be absorbed and utilized by the light absorbers.

iii. Improvement of FF: The passivator can enhance interlayer interactions between different layers with the PSC devices, minimizing energy losses and improving charge carrier transport.

Table 1. Summary of the function of the different passivators for specific perovskite materials on the open-circuit voltage (VOC), short-circuit current density (JSC), fill factor (FF) and long-term stability (LST) with the corresponding exchange-correlation (XC) functionals

Perovskite	Passivator(s)	XC	V_{OC}	J_{SC}	FF	LTS	Ref.
$CsPbI_3$	Benzoyl hydrazine	PBE, D3	2.6%	1.9%	1.6%	√	[84]
$Rb_{0.05}Cs_{0.05}(FA_{0.83}MA_{0.17})Pb(I_{0.83}Br_{0.17})_3$	acetylcholine	PBE	8.0%		3.8%	√	[85]
$(FAPbI_3)_{0.95}(MAPbBr_3)_{0.05}$	chlorobenzenesulfonic potassium salts	PBE, D3	5.7%			√	[86]
$MAPbI_3$	Single-walled carbon nanotubes	PBE	8.0%	23%		√	[87]
$Rb_{0.05}Cs_{0.05}MA_{0.05}FA_{0.85}Pb(I_{0.95}Br_{0.05})_3$	3-(amino methyl) pyridine	GGA	3.8%	1.6%	3.6%	√	[89]
$MAPbI_3$	Cs-doped $Ti_3C_2T_x$	optB86b	2.7%	3.9%	7.0%	√	[90]
$CsPbI_{3-x}Br_x$	Boc-S-4-methoxy-benzyl-L-cysteine	PBE	9.2%	2.8%	4.4%	√	[91]
$CsPbI_{3-x}Br_x$	trifluoroacetamidine	PBE	3.5%	2.5%	5.3%	√	[92]
$CsPbI_{3-x}Br_x$	4-Fluorophenethyl ammonium, 4-(Trifluoromethyl) phenethylammonium	B3LYP, HES, D3	19%	2.3%	4.4%	√	[97]
$CsPbI_{3-x}Br_x$	2-mercapto-1-methylimidazole	PBE	11%		2.8%	√	[98]
$Cs_{0.1}FA_{0.9}$ PbI_3	Sb dopants In dopants	PBE, D3	7.8%	14%	17%		[99]
$FAPbI_3$	bathocuproine	PBE, D3	1.2%	3.5%	3.1%	√	[102]
$MAPbI_3$	tris(2,4,6-trichloro phenyl) methyl	PBE, D3	3.7%	5.1%	4.5%	√	[103]
$(FAPbI_3)_{0.95}(MAPbBr_3)_{0.05}$	OATsO	PBEsol, D3	4.9%		4.9%	√	[104]
$MAPbI_3$	TEA	optB86b, vdW-DF				√	[105]
$CsPbI_2Br$	dithiocarbamate	GGA, D3, SOC	13%		4.2%	√	[106]

iv. Enhancement of stability: LTS and resistance to degradation are crucial, ensuring the passivator maintains its effectiveness throughout the lifetime of PSCs. Passivators should have stronger binding strength with the light absorbers to provide a protective barrier to safeguard the perovskite material.

The passivation process is important as it can improve the critical parameters associated with the best PSC efficiency. The combined effectiveness of these properties determines a successful passivator. The examples in this review are summarized in Table 1, showing that passivators can improve V_{OC}, J_{SC}, and FF to some extent. Some passivators can have a specific impact on a specific parameter, and all of them can significantly enhance the LTS. DFT studies can provide a theoretical explanation of these improvements. To understand the different influences of passivators, corresponding XC functionals were used with the compromise between the computational cost and accuracy.

While the computational results can reproduce a qualitative trend along with the experimental observations, which were provided throughout this review, the theoretical results cannot provide a quantitative comparison with the experimental data due to the oversimplified models used in theoretical studies without the consideration of most of the working conditions. Additionally, while DFT-based calculation methods offer a means to uncover atomic-level details of passivation within the solar cell systems, the extension of the molecular-scale models to macroscopic descriptions related to solar-to-electricity processes is required. For example, the grain effect in systems with large numbers of atoms and small grains can result in increased surface area and surface states that require consideration. Consequently, a multi-scale simulation approach is required, encompassing atomic-level quantum states and the macroscopic observations of passivation technologies. There are two main categories of multi-scale simulation approaches: concurrent and sequential. Concurrent multi-scale modeling involves directly applying multiple levels of theory in a

single simulation, explicitly capturing phenomena occurring across various time and length scales. A common example of concurrent coupling in electrochemistry is quantum mechanics/molecular mechanics (QM/MM) modeling, where the electronic structure method describes a small portion of reactions while molecular force fields are employed for the dynamical part. In contrast, sequential multi-scale modeling involves using results from one level of modeling as input for another level, allowing subsequent simulations to overcome the time and length scale limitations of the parent model. This approach, known as parameter passing, enables more flexibility in the simulations. It is important to note that while these approaches offer computational efficiency, there are trade-offs to consider.

DECLARATIONS

Authors' contributions

Conceptualization, investigation, methodology, validation, formal analysis, writing, reviewing, and editing: Allen OJ
Methodology, validation, formal analysis, writing, reviewing, and editing: Kang J
Figure generation, validation, formal analysis: Qian S
Writing, reviewing, and editing: Zhang L, Hinsch JJ
Conceptualization, validation, supervision, writing, reviewing, and editing: Wang Y

Availability of data and materials

Not applicable.

Financial support and sponsorship

The authors acknowledge financial support from Griffith University (CEE2550), the Australian Research Council Discovery Project (Grant No. DP210103266), and the Discovery Early Career Researcher Award (DE240101090).

Conflicts of interest

All authors declared that there are no conflicts of interest.

Ethical approval and consent to participate

Not applicable.

Consent for publication

Not applicable.

REFERENCES

1. Jesper Jacobsson T, Correa-baena J, Pazoki M, et al. Exploration of the compositional space for mixed lead halogen perovskites for high efficiency solar cells. *Energy Environ Sci* 2016;9:1706-24. DOI
2. Park N. Perovskite solar cells: an emerging photovoltaic technology. *Mater Today* 2015;18:65-72. DOI
3. Tan Q, Li Z, Luo G, et al. Inverted perovskite solar cells using dimethylacridine-based dopants. *Nature* 2023;620:545-51. DOI
4. Yang Z, Zhang W, Wu S, et al. Slot-die coating large-area formamidinium-cesium perovskite film for efficient and stable parallel solar module. *Sci Adv* 2021;7:eabg3749. DOI PubMed PMC

5. Yang F, Jang D, Dong L, et al. Upscaling solution-processed perovskite photovoltaics. *Adv Energy Mater* 2021;11:2101973. DOI
6. Gao F, Zhao Y, Zhang X, You J. Recent progresses on defect passivation toward efficient perovskite solar cells. *Adv Energy Mater* 2020;10:1902650. DOI
7. Ball JM, Petrozza A. Defects in perovskite-halides and their effects in solar cells. *Nat Energy* 2016;1:16149. DOI
8. You S, Eickemeyer FT, Gao J, et al. Bifunctional hole-shuttle molecule for improved interfacial energy level alignment and defect passivation in perovskite solar cells. *Nat Energy* 2023;8:515-25. DOI
9. Meng L, You J, Yang Y. Addressing the stability issue of perovskite solar cells for commercial applications. *Nat Commun* 2018;9:5265. DOI PubMed PMC
10. Wang R, Mujahid M, Duan Y, Wang Z, Xue J, Yang Y. A review of perovskites solar cell stability. *Adv Funct Mater* 2019;29:1808843. DOI
11. Li Z, Li B, Wu X, et al. Organometallic-functionalized interfaces for highly efficient inverted perovskite solar cells. *Science* 2022;376:416-20. DOI
12. Abdi-Jalebi M, Andaji-Garmaroudi Z, Cacovich S, et al. Maximizing and stabilizing luminescence from halide perovskites with potassium passivation. *Nature* 2018;555:497-501. DOI
13. Zhan Y, Yang F, Chen W, et al. Elastic lattice and excess charge carrier manipulation in 1D-3D Perovskite solar cells for exceptionally long-term operational stability. *Adv Mater* 2021;33:e2105170. DOI
14. Luo L, Zeng H, Wang Z, et al. Stabilization of 3D/2D perovskite heterostructures via inhibition of ion diffusion by cross-linked polymers for solar cells with improved performance. *Nat Energy* 2023;8:294-303. DOI
15. Li Y, Liu L, Zheng C, et al. Plant-derived l -theanine for ultraviolet/ozone resistant perovskite photovoltaics. *Adv Energy Mater* 2023;13:2203190. DOI
16. Park J, Kim J, Yun HS, et al. Controlled growth of perovskite layers with volatile alkylammonium chlorides. *Nature* 2023;616:724-30. DOI
17. Li M, Sun R, Chang J, et al. Orientated crystallization of FA-based perovskite via hydrogen-bonded polymer network for efficient and stable solar cells. *Nat Commun* 2023;14:573. DOI PubMed PMC
18. Zhang Z, Qiao L, Meng K, Long R, Chen G, Gao P. Rationalization of passivation strategies toward high-performance perovskite solar cells. *Chem Soc Rev* 2023;52:163-95. DOI PubMed
19. Xia J, Liang C, Gu H, et al. Surface passivation toward efficient and stable perovskite solar cells. *Energy Environ Mater* 2023;6:e12296. DOI
20. Azaid A, Kacimi R, Alaqarbeh M, et al. Design of a D-Di-π-A architecture with different auxiliary donors for dye-sensitized solar cells: density functional theory/time-dependent-density functional theory study of the effect of secondary donors. *Advcd Theory Sims* 2023;6:2300054. DOI
21. Hassan T, Adnan M, Hussain R, Hussain F, Khan MU. Molecular engineering of Pyran-fused acceptor-donor-acceptor-type non-fullerene acceptors for highly efficient organic solar cells - a density functional theory approach. *J Phys Org Chem* 2023;36:e4507. DOI
22. Kagdada HL, Roondhe B, Roondhe V, et al. Exploring a-site cation variations in dion-jacobson two-dimensional halide perovskites for enhanced solar cell applications: a density functional theory study. *Adv Energy Sustain Res* 2024;5:2300147. DOI
23. Saloni S, Ranjan P, Chakraborty T. A computational study of $CuCrX_2$ (X = S, Se, Te) for intermediate band solar cell: conceptual density functional theory approach. *J Mol Graph Model* 2023;124:108534. DOI
24. Setsoafia DDY, Ram KS, Mehdizadeh-rad H, Ompong D, Singh J. Density functional theory simulation of optical and photovoltaic properties of DRTB-T donor-based organic solar cells. *Int J Energy Res* 2023;2023:1-12. DOI
25. Srivastava A, Lenka TR, Anthoniappen J, Tripathy SK. Investigation on thermodynamic properties of novel $Ag_2SrSn(S/Se)_4$ quaternary chalcogenide for solar cell applications: a density functional theory study. In: Lenka TR, Misra D, Fu L, editors. Micro and nanoelectronics devices, circuits and systems. Singapore: Springer Nature; 2023. pp. 103-10. DOI
26. Taouali W, Alimi K, Sindhoo Nangraj A, Casida ME. Density-functional theory (DFT) and time-dependent DFT study of the chemical and physical origins of key photoproperties of end-group derivatives of a nonfullerene acceptor molecule for bulk heterojunction organic solar cells. *J Comput Chem* 2023;44:2130-48. DOI
27. Kaiser W, Carignano M, Alothman AA, et al. First-principles molecular dynamics in metal-halide perovskites: contrasting generalized gradient approximation and hybrid functionals. *J Phys Chem Lett* 2021;12:11886-93. DOI
28. Ohto T, Dodia M, Imoto S, Nagata Y. Structure and dynamics of water at the water-air interface using first-principles molecular dynamics simulations within generalized gradient approximation. *J Chem Theory Comput* 2019;15:595-602. DOI
29. Pandech N, Kongnok T, Palakawong N, Limpijumnong S, Lambrecht WRL, Jungthawan S. Effects of the van der Waals interactions on structural and electronic properties of $CH_3NH_3(Pb,Sn)(I,Br,Cl)_3$ halide perovskites. *ACS Omega* 2020;5:25723-32. DOI PubMed PMC
30. Wang Y, de Gironcoli S, Hush NS, Reimers JR. Successful a priori modeling of CO adsorption on Pt(111) using periodic hybrid density functional theory. *J Am Chem Soc* 2007;129:10402-7. DOI PubMed

31. Gusakova J, Wang X, Shiau LL, et al. Electronic properties of bulk and monolayer TMDs: theoretical study within DFT framework (GVJ-2e Method). *Physica Status Solidi* 2017;214:1700218. DOI
32. Borlido P, Aull T, Huran AW, Tran F, Marques MAL, Botti S. Large-scale benchmark of exchange-correlation functionals for the determination of electronic band gaps of solids. *J Chem Theory Comput* 2019;15:5069-79. DOI PubMed PMC
33. Wang Y, Zhang H, Liu P, Yao X, Zhao H. Engineering the band gap of bare titanium dioxide materials for visible-light activity: a theoretical prediction. *RSC Adv* 2013;3:8777-82. DOI
34. Zaki NH, Ali AMM, Mohamad Taib MF, Wan Ismail WIN, Sepeai S, Ramli A. Dispersion-correction density functional theory (DFT+D) and spin-orbit coupling (SOC) method into the structural, electronic, optical and mechanical properties of CH3NH3PbI3. *Comput Condens Matter* 2023;34:e00777. DOI
35. Shi T, Yin W, Hong F, Zhu K, Yan Y. Unipolar self-doping behavior in perovskite $CH_3NH_3PbBr_3$. *Appl Phys Lett* 2015;106:103902. DOI
36. Huang Y, Sun QD, Xu W, He Y, Yin WJ. Halide perovskite materials for solar cells: a theoretical review. *Acta Phys Sin* 2017;33:1730-51. DOI
37. Yin W, Yang J, Kang J, Yan Y, Wei S. Halide perovskite materials for solar cells: a theoretical review. *J Mater Chem A* 2015;3:8926-42. DOI
38. Amat A, Mosconi E, Ronca E, et al. Cation-induced band-gap tuning in organohalide perovskites: interplay of spin-orbit coupling and octahedra tilting. *Nano Lett* 2014;14:3608-16. DOI
39. Bhattacharya S, Kanai Y. Spin-orbit-coupling-induced band splitting in two-dimensional hybrid organic-inorganic perovskites: Importance of organic cations. *Phys Rev Mater* 2023;7:055001. DOI
40. Ronca E, De Angelis F, Fantacci S. Time-dependent density functional theory modeling of spin-orbit coupling in ruthenium and osmium solar cell sensitizers. *J Phys Chem C* 2014;118:17067-78. DOI
41. Even J, Pedesseau L, Jancu J, Katan C. Importance of spin-orbit coupling in hybrid organic/inorganic perovskites for photovoltaic applications. *J Phys Chem Lett* 2013;4:2999-3005. DOI
42. Idrissi S, Labrim H, Bahmad L, Benyoussef A. DFT and TDDFT studies of the new inorganic perovskite CsPbI3 for solar cell applications. *Chem Phys Lett* 2021;766:138347. DOI
43. Das T, Di Liberto G, Pacchioni G. Density functional theory estimate of halide perovskite band gap: when spin orbit coupling helps. *J Phys Chem C* 2022;126:2184-98. DOI
44. Alsalamah IM, Shaari A, Alsaif NA, Yamusa SA, Lakshminarayana G, Rekik N. Exploring the structural properties and the optoelectronic features of $RbPbX_3$ (X = Cl, F) perovskite crystals for solar cells solicitations: showcasing the DFT predictions. *Chem Phys* 2023;573:111978. DOI
45. Borges-martínez M, Saavedra-torres M, Schott E, Zarate X. Computational design and properties elucidation of new $(FAPbI_3)_{1-x-y}(MAPbBr_3)_y(CsPbBr_3)_x$ photoactive systems for their application in perovskite solar cells. *Mater Today Commun* 2023;34:105324. DOI
46. Arfaoui Y, Khenfouch M, Habiballah N. A DFT and time-dependent DFT investigation of the structural, electronic and optical properties of lead-free FAMgI3 perovskite for photovoltaic applications. *J Electron Mater* 2024;53:881-90. DOI
47. Glockzin B, Oakley MS, Karmakar A, et al. Alkali tin halides: exploring the local structure of A_2SnX_6 (A = K, Rb; X = Cl, Br, I) compounds using solid-state NMR and DFT computations. *J Phys Chem C* 2023;127:7284-98. DOI
48. Graupner DR, Kilin DS. Size effects on polaron formation in lead chloride perovskite thin films. *Mol Phys* 2023. DOI
49. Haroon M, Baig MW, Akhtar T, Tahir MN, Ashfaq M. Relativistic two-component time dependent density functional studies and Hirshfeld surface analysis of halogenated arylidenehydrazinylthiazole derivatives. *J Mol Structure* 2023;1287:135692. DOI
50. Idrissi S, Mounkachi O, Bahmad L, Benyoussef A. Study of the solar perovskites: $XZnF_3$ (X = Ag, Li or Na) by DFT and TDDFT methods. *J Korean Ceram Soc* 2023;60:424-33. DOI
51. Islam MR, Mazumder AAM, Mojumder MRH, Shifat ASMZ, Hossain MK. Strain-induced tunable optoelectronic properties of inorganic halide perovskites $APbCl_3$ (A = K, Rb, and Cs). *Jpn J Appl Phys* 2023;62:011002. DOI
52. Javed M, Sattar MA, Benkraouda M, Amrane N, Najar A. Strained induced metallic to semiconductor transitions in 2D Ruddlesden Popper perovskites: a GGA + SOC approach. *Appl Surf Sci* 2023;627:157244. DOI
53. Kumar D, Chand P. Enhanced optical and thermoelectric properties of Ti doped half - Heusler alloy NbRuP: a first principles study. *Solid State Commun* 2023;366-7:115179. DOI
54. Kumar G, Ravidas BK, Bhattarai S, Roy MK, Samajdar DP. Exploration of the photovoltaic properties of oxide-based double perovskite Bi_2FeCrO_6 using an amalgamation of DFT with spin-orbit coupling effect and SCAPS-1D simulation approaches. *New J Chem* 2023;47:18640-58. DOI
55. Laghzaoui S, Lamrani AF, Laamara RA. Robust half-metallic ferromagnet in doped double perovskite Sr_2TiCoO_6 by rare-earth elements for photovoltaic and thermoelectric conversion: a DFT method. *J Phys Chem Solid* 2023;183:111639. DOI
56. Li S, Chen Y, Wang Z, et al. Theoretical studies of new iridium-based terpolymer donors for high-efficiency triplet-material-based organic photovoltaics: Incorporation of different iridium(III) complexes. *Mater Chem Phys* 2023;302:127780. DOI
57. Moaddeli M, Kanani M, Grünebohm A. Electronic and structural properties of mixed-cation hybrid perovskites studied using an efficient spin-orbit included DFT-1/2 approach. *Phys Chem Chem Phys* 2023;25:25511-25. DOI PubMed
58. Mokkath J. Tailoring the infrared resonances of sulfide perovskites. *Mater Today Chem* 2023;30:101589. DOI
59. Muthumari M, Manjula M, Veluswamy P, Kuznetsov DV. First principles calculations to investigate structural, electronic, mechanical, thermoelectric and optical properties of Bi- and Se-doped SnTe. *J Phys Chem Solid* 2023;176:111232. DOI

60. Rahman MF, Rahman MA, Islam MR, et al. Unraveling the strain-induced and spin-orbit coupling effect of novel inorganic halide perovskites of Ca_3AsI_3 using DFT. *AIP Adv* 2023;13:085329. DOI
61. Raju N, Tripathi D, Lahiri S, Thangavel R. Heat reflux sonochemical synthesis of Cu_3BiS_3 quantum dots: experimental and first-principles investigation of spin-orbit coupling on structural, electronic, and optical properties. *Solar Energy* 2023;259:107-18. DOI
62. Supatutkul C, Sitarachu K, Laosiritaworn Y, Jaroenjittichai AP. Quasiparticle band structures of $Cs_2B^+B^{3+}Br_6$ lead-free halide double perovskites. *Mater Today Commun* 2023;36:106751. DOI
63. Yami NFNA, Ramli A, Nawawi WI, et al. Structural, electronic, and optical properties of lower-dimensional hybrid perovskite lead-iodide frameworks + SOC via density functional theory. *Emergent Mater* 2023;6:999-1007. DOI
64. Liu J, Kang J, Chen S, et al. Effects of compositional engineering and surface passivation on the properties of halide perovskites: a theoretical understanding. *Phys Chem Chem Phys* 2020;22:19718-24. DOI
65. Heyd J, Scuseria GE, Ernzerhof M. Erratum: "Hybrid functionals based on a screened Coulomb potential". *J Chem Phys* 2006;124:219906. DOI
66. West AR. Solid state chemistry and its applications. 2nd ed. Hoboken: John Wiley & Sons; 2022.
67. Zhilyakov LA, Kostanovskii AV, Pokhil GP. Condition of formation of 2D coulomb crystal on the surface of dielectric. *High Temp* 2008;46:721-4. DOI
68. Umari P, Mosconi E, De Angelis F. Relativistic GW calculations on $CH_3NH_3PbI_3$ and $CH_3NH_3SnI_3$ perovskites for solar cell applications. *Sci Rep* 2014;4:4467. DOI PubMed PMC
69. Li H, Shi J, Deng J, et al. Intermolecular π-π conjugation self-assembly to stabilize surface passivation of highly efficient perovskite solar cells. *Adv Mater* 2020;32:e1907396. DOI
70. Zheng Y, Zhang S, Ma J, et al. Codependent failure mechanisms between cathode and anode in solid state lithium metal batteries: mediated by uneven ion flux. *Sci Bull* 2024;69:317-9. DOI
71. Zhao H, Kordas K, Ojala S. Recent advances in synthesis of water-stable metal halide perovskites and photocatalytic applications. *J Mater Chem A* 2023;11:22656-87. DOI
72. Goyal A, Singh PP, Mondal T. Investigating the role of Co and Fe in bimetallic perovskite catalysts ($LaNiO_3$) for steam reforming of Bio-Oil model oxygenates: a DFT study. *Carbon* 2023;2:2.606. Available from: https://oxford-abstracts.s3.amazonaws.com/f0e3a240-bf65-43be-8a7c-c42d93fa4e3e.pdf [Last accessed on 22 Apr 2024].
73. Bayendang NP, Kahn MT, Balyan V. Thermoelectric generators (TEGs) modules-optimum electrical configurations and performance determination. *AIMS Energy* 2022;10:102-30. DOI
74. Imai Y, Nishizawa S, Ito K. Reduction of LSI maximum power consumption with standard cell library of stack structured cells. *IEICE Trans Fund* 2022;E105.A:487-96. DOI
75. Keller J, Aboulfadl H, Stolt L, Donzel-gargand O, Edoff M. Rubidium fluoride absorber treatment for wide-gap (Ag,Cu)(In,Ga)Se_2 solar cells. *Solar RRL* 2022;6:2200044. DOI
76. Kulkarni V, Ghaisas G, Krishnan S. Performance analysis of an integrated battery electric vehicle thermal management. *J Energy Stor* 2022;55:105334. DOI
77. Okedu KE, Al Ghaithi ASS. Comparative study of the internal dynamic failures of grid-connected solar PVs: the case of the oman power network. *Front Energy Res* 2022;10:858803. DOI
78. Mozaffari S, Kiamehr Z. A theoretical study on internal losses of heat generation in inorganic metal oxide charge transporting layers-based inverted PSC. *Opt Quant Electron* 2023;55:826. DOI
79. Li H, Shi P, Wang L, et al. Cooperative catalysis of polysulfides in lithium-sulfur batteries through adsorption competition by tuning cationic geometric configuration of dual-active sites in spinel oxides. *Angew Chem Int Ed* 2023;62:e202216286. DOI
80. Xia J, Sohail M, Nazeeruddin MK. Efficient and stable perovskite solar cells by tailoring of interfaces. *Adv Mater* 2023;35:e2211324. DOI PubMed
81. Pratheek M, Abhinav T, Bhattacharya S, Chandra GK, Predeep P. Recent progress on defect passivation in perovskites for solar cell application. *Mater Sci Energy Technol* 2021;4:282-9. DOI
82. Zhu R, Guan N, Wang D, Bao Y, Wu Z, Song L. Review of defect passivation for NiO_x-based inverted perovskite solar cells. *ACS Appl Energy Mater* 2023;6:2098-121. DOI
83. Zhang Y, Liu Y, Liu S. Composition engineering of perovskite single crystals for high-performance optoelectronics. *Adv Funct Mater* 2023;33:2210335. DOI
84. Che Y, Liu Z, Duan Y, et al. Hydrazide derivatives for defect passivation in pure $CsPbI_3$ Perovskite Solar Cells. *Angew Chem Int Ed* 2022;61:e202205012. DOI
85. Zhang Z, Jiang J, Xiao Liu X, et al. Surface-anchored acetylcholine regulates band-edge states and suppresses ion migration in a 21% -efficient quadruple-cation perovskite solar cell. *Small* 2022;18:e2105184. DOI
86. Dong Y, Shen W, Dong W, et al. Chlorobenzenesulfonic potassium salts as the efficient multifunctional passivator for the buried interface in regular perovskite solar cells. *Adv Energy Mater* 2022;12:2200417. DOI
87. Batmunkh M, Macdonald TJ, Shearer CJ, et al. Carbon nanotubes in TiO_2 nanofiber photoelectrodes for high-performance perovskite solar Cells. *Adv Sci* 2017;4:1600504. DOI PubMed PMC
88. Chavan RD, Parikh N, Tavakoli MM, et al. Band alignment and carrier recombination roles on the open circuit voltage of ETL-passivated perovskite photovoltaics. *Intl J Energy Res* 2022;46:6022-30. DOI
89. Jiang Q, Tong J, Xian Y, et al. Surface reaction for efficient and stable inverted perovskite solar cells. *Nature* 2022;611:278-83. DOI

90. Bati AS, Sutanto AA, Hao M, et al. Cesium-doped $Ti_3C_2T_x$ MXene for efficient and thermally stable perovskite solar cells. *Cell Rep Phys Sci* 2021;2:100598. DOI
91. Zhang H, Tian Q, Xiang W, et al. Tailored cysteine-derived molecular structures toward efficient and stable inorganic perovskite solar cells. *Adv Mater* 2023;35:e2301140. DOI
92. Zhang H, Xiang W, Zuo X, et al. Fluorine-containing passivation layer via surface chelation for inorganic perovskite solar cells. *Angew Chem Int Ed* 2023;62:e202216634. DOI
93. Batmunkh M, Vimalanathan K, Wu C, et al. Efficient production of phosphorene nanosheets via shear stress mediated exfoliation for low-temperature perovskite solar cells. *Small Method* 2019;3:1800521. DOI
94. Macdonald TJ, Clancy AJ, Xu W, et al. Phosphorene nanoribbon-augmented optoelectronics for enhanced hole extraction. *J Am Chem Soc* 2021;143:21549-59. DOI
95. Allen OJ, Kang J, Wang Y. First-principles study of group VA monolayer passivators for perovskite solar cells. *ACS Appl Nano Mater* 2023;6:4279-87. DOI
96. Cheng L, Zhang C, Liu Y. The Optimal electronic structure for high-mobility 2D semiconductors: exceptionally high hole mobility in 2D antimony. *J Am Chem Soc* 2019;141:16296-302. DOI
97. Li T, Xu J, Lin R, et al. Inorganic wide-bandgap perovskite subcells with dipole bridge for all-perovskite tandems. *Nat Energy* 2023;8:610-20. DOI
98. Xu T, Xiang W, Yang J, et al. Interface modification for efficient and stable inverted inorganic perovskite solar cells. *Adv Mater* 2023;35:e2303346. DOI
99. Qiao HW, Yang S, Wang Y, et al. A gradient heterostructure based on tolerance factor in high-performance perovskite solar cells with 0.84 fill factor. *Adv Mater* 2019;31:e1804217. DOI
100. Zhang B, Oh J, Sun Z, et al. Buried guanidinium passivator with favorable binding energy for perovskite solar cells. *ACS Energy Lett* 2023;8:1848-56. DOI
101. Liu Q, Wu Y, Li D, et al. Dilute alloying to implant activation centers in nitride electrocatalysts for lithium-sulfur batteries. *Adv Mater* 2023;35:e2209233. DOI
102. Fei C, Li N, Wang M, et al. Lead-chelating hole-transport layers for efficient and stable perovskite minimodules. *Science* 2023;380:823-9. DOI
103. Xie P, Xiao H, Qiao Y, et al. Radical reinforced defect passivation strategy for efficient and stable $MAPbI_3$ perovskite solar cells fabricated in air using a green anti-solvent process. *Chem Eng J* 2023;462:142328. DOI
104. Tan S, Huang T, Yavuz I, et al. Stability-limiting heterointerfaces of perovskite photovoltaics. *Nature* 2022;605:268-73. DOI
105. Yang S, Wang Y, Liu P, Cheng Y, Zhao HJ, Yang HG. Functionalization of perovskite thin films with moisture-tolerant molecules. *Nat Energy* 2016;1:15016. DOI
106. He J, Liu J, Hou Y, Wang Y, Yang S, Yang HG. Surface chelation of cesium halide perovskite by dithiocarbamate for efficient and stable solar cells. *Nat Commun* 2020;11:4237. DOI PubMed PMC
107. Zhang L, Lin S, Wu B, Li Q, Li J. Understanding structures and properties of phosphorene/perovskite heterojunction toward perovskite solar cell applications. *J Mol Graph Model* 2019;89:96-101. DOI